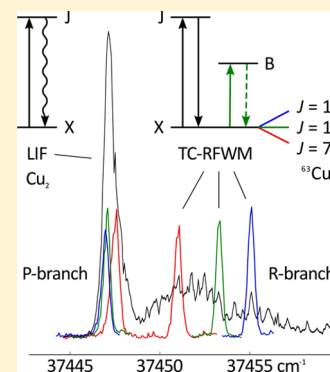


Rovibrational Characterization of High-Lying Electronic States of Cu_2 by Double-Resonant Nonlinear SpectroscopyM. Beck,[†] B. Visser,[†] P. Bornhauser,[†] G. Knopp,[†] J. A. van Bokhoven,^{‡,§} and P. P. Radi^{*,†}[†]SwissFEL, Paul Scherrer Institute, 5232 Villigen PSI, Switzerland[‡]Energy and Environment Research Division, Paul Scherrer Institute, 5232 Villigen PSI, Switzerland[§]Department of Chemistry and Applied Biosciences, ETH Zurich, 8093 Zürich, Switzerland

Supporting Information

ABSTRACT: The available knowledge of the electronically excited states of the copper dimer is limited. This is common for transition metals, as the high density of states hinders both experimental assignment and computation. In this work, two-color resonant four-wave mixing spectroscopy was applied to neutral Cu_2 in the gas phase. The method yielded accurate positions of individual rovibrational lines in the I-X and J-X electronic systems. This revealed the term symbols for the I and J states as $^1\Pi_u(1_u)$ and $^1\Sigma_u^+(0_u^+)$, respectively. For the $^{63}\text{Cu}_2$ isotopologue, accurate molecular constants were obtained. The characterization of the J state finally allowed decisive determination of its electron configuration. The J state is obtained from the ground state by promotion of a $3d\pi_g$ electron into the weakly bonding $4p\pi_u$ molecular orbital. From the data analysis, lifetimes of the I state (between 10 ps and 5 ns) and J state (66 ns) were inferred.



INTRODUCTION

Transition metal atoms, dimers, and small clusters have unique properties and are crucial in fields like catalysis, optoelectronics, and nanophotonics. However, the electronic states responsible for these properties are barely known. The high density of states, which arises from the many configurations with partly filled d subshells, has thus far hindered both computational and spectroscopic assignment of the excited states and their interactions. The high reactivity of such species complicates experimental studies further, especially for neutral species that cannot be trapped and mass-selected by electric and magnetic fields. Mass selection is crucial, as the properties of small clusters do not scale with number of atoms. For dimers and the smallest clusters, quantum effects are dominant. To disentangle and characterize the individual electronic states of such species, cluster production, mass selection, and spectral simplification need to be achieved at the same time.

The copper dimer has one of the simplest electronic systems among the transition metals. Cu_2 is of large interest due to its role as an active site in both heterogeneous catalysis¹ and metalloenzymes.^{2,3} Nevertheless, only a few excited electronic states are fully characterized spectroscopically. While the ground state of Cu_2 is well-separated from other low-lying states, the situation dramatically changes on electronic excitation. The d-holes, which are generated as a result, yield a high density of states in the elevated energy range. Consequently, the aforementioned challenges emerge. The overlapping and perturbing bands can render assignment of single lines almost impossible, and most quantum chemical *ab initio* methods fail.

A comprehensive overview on the experimental work on the copper dimer was given by Morse in 1993.⁴ Since then, only a limited amount of data has been added, mostly from low-resolution detection of bands in the UV.^{5,6} Recently, resonant two-color spectroscopy was used by Perry et al. to label neutral Cu_2 while studying its photoionization dynamics.⁷

The I and the J states of Cu_2 were initially detected using resonant two-photon ionization (R2PI) with mass-selective detection.⁸ The method allowed isotopologue-selective assignment of the lowest vibrational levels of the J state and some vibrationally excited levels of the I state. For the J state, rotational constants were obtained by use of laser-induced fluorescence (LIF).⁹ However, these spectra were not sufficiently resolved to determine the term symbol of the J state. Since the I state was not observed by the LIF measurements, no rotational constants were obtained.

Two-color resonant four-wave mixing (TC-RFWM), used as a spectroscopic technique, combines the spectral simplification of double-resonant methods with background-free detection. Three incident laser beams of two wavelengths are superimposed at a very acute angle. In the optically thin medium of a molecular beam, nonlinear interaction of these beams is only observable if all wavelengths are in resonance with transitions in a unique species. Furthermore, these rovibronic transitions need to possess a common state. If these conditions are fulfilled, a laser-like signal beam is generated in a fourth

Received: October 4, 2017

Revised: October 13, 2017

Published: October 16, 2017

direction, which is governed by phase-matching conditions. By tuning one wavelength to a single rovibronic transition of a target species, a scan of the second wavelength will only exhibit optically allowed transitions that are connected to rovibronic states addressed by the tuned transition. A more comprehensive introduction into TC-RFWM can be found in our initial study on Cu_2 , where we used the well-characterized A-X and B-X transitions to verify our setup.¹⁰ There, we demonstrated the applicability of TC-RFWM within the molecular beam expansion of a metal cluster source and its capability to obtain isotopologue pure spectra of Cu_2 from a metal target of natural abundance.

Here, we utilize the TC-RFWM method to determine the term symbols and the molecular constants of the high-lying I and J states. On the basis of selection rules, the term symbols of these states can be directly deduced from the presence or absence of a Q branch in the I-X and J-X transitions, respectively. A series of unperturbed transitions was sought for straightforward fitting of the molecular constants. In the spectral range studied, unperturbed transitions were only observed for the lighter $^{63}\text{Cu}_2$ isotopologue. For the heavier $^{63}\text{Cu}^{65}\text{Cu}$ isotopologue, the observed bands are strongly perturbed by multiple crossing states. To obtain molecular constants for the latter, additional data and a full deperturbation study are necessary and omitted in this work. The minor $^{65}\text{Cu}^{65}\text{Cu}$ isotopologue was not observable due to the squared dependency of the method with respect to the number density of the target species. In addition to TC-RFWM, the simultaneous collection of dispersed LIF allowed the determination of the lifetimes of the unperturbed I and J states.

■ EXPERIMENTAL METHODS

The experimental setup is in large part as previously reported,¹⁰ though some details in the following overview have been updated as the cluster source prototype in use has matured. The copper dimers are produced by a home-built laser-ablation source, situated inside a vacuum chamber. A pulsed valve (Series 9 General Valve, Parker-Hannifin) emits pulses of helium (grade 6.0, 23 bar backing pressure) into a cylindrical channel of 2 mm diameter. After 9 cm, one side of the channel extends to expose the surface of a copper target (standard sputter target disk, 50 mm \times 3 mm, 99.95% Cu). This target is rotated and translated about 0.1 mm behind the body containing the channel. A PEEK seal minimizes gas loss between target and body. The ablation laser pulses (532 nm, 10 ns, 100 mJ) enter the gas channel from the opposite side through a small hole and hit the target perpendicularly to the surface. To avoid excessive gas loss on the laser entry side, a (black) aluminum foil is clamped over the hole. A small pinhole is created in the foil by the ablation laser (focused by an $f = 500$ mm lens). Upon ablation, the plume of copper plasma is entrained in the helium pulse and propagates through the gas channel. Cooling and condensation takes place in the confined channel for about 8.5 cm beyond the ablation spot. Subsequently, the helium pulse, carrying the copper dimers and small clusters, is expanded into high vacuum. In this process further cooling takes place, and a collision-free molecular beam is created in the so-called quiet zone of the supersonic expansion.

The optical TC-RFWM spectroscopy is performed 1 cm downstream from the nozzle, where the density of the neutral copper dimers remains high and no collisional broadening of

the spectra occurs. Three incident, parallel propagating laser beams are focused through a quartz window into this region by a lens (2 in. diameter, $f = 1000$ mm). The distance from the optical axis is used to adjust the relative angles of the beams at the focal point and thereby the phase-matching condition. The signal beam exits the vacuum chamber through a second window and is collimated by a lens (2 in. diameter, $f = 1000$ mm). After 3 m of additional optical path, detection is performed by focusing the signal beam through a pinhole onto a photomultiplier tube. This extended beam path largely reduces signal contributions by isotropically emitted fluorescence, which would add a LIF background to the otherwise background-free method. The incident laser beams are produced using Nd:YAG (third harmonic) pumped dye lasers (NarrowScan, Radiant Dyes, 0.04 cm^{-1} specified line width) and second harmonic generation for producing the ultraviolet beams needed for the I-X and J-X transitions ($\sim 100 \mu\text{J}/\text{pulse}$). Double-resonant selection of individual rotational quantum numbers in the ground state was mostly achieved by tuning the probe dye laser to transitions in the (1–0) B-X band. This electronic system is chosen because of its high transition strength (requiring $<100 \text{ nJ}/\text{pulse}$), and the (1–0) band is advantageous due to the larger isotopic splitting as compared to the (0–0) band. The frequency-doubled laser beam is split to provide the third incident beam needed for four-wave mixing. For this work, the spectra were recorded with a wavelength step size of 0.5 pm before frequency doubling, resulting in wavenumber steps of about 0.035 cm^{-1} . At this step size, the wavelength steps of the dye lasers were no longer equidistant. Therefore, the wavelengths corresponding to each data point were measured using a wavelength meter (WS 6, HighFinesse/Ångström).

To provide an additional channel of information, a spherical mirror is placed perpendicularly to both molecular beam and the main axis of spectroscopy. The collected light is focused onto the slit of a 1 m monochromator (SPEX) in front of a photomultiplier tube. In this work the usage of dispersed LIF was limited to the measurement of lifetimes.

■ RESULTS AND DISCUSSION

Figure 1 shows example TC-RFWM spectra, with the applied double-resonant scheme shown in the inset. The probe wavenumbers in the (1–0) B-X band are calculated on the basis of the molecular constants from Ram et al.¹¹ Good agreement of these constants with the results obtained by applying our setup has been demonstrated previously.¹⁰ The pump wavenumbers were scanned over the bands of interest. To the left, the (“x+1”–0) I-X band is shown, and to the right, the neighboring (0–0) J-X band is shown. The vibrational numbering of the I state is not known; therefore, the labeling used by Powers et al.⁸ is adopted, where x represents the lowest experimentally known vibrational state. At the top, the fluorescence emission of an excitation scan to the first vibrationally excited level of the electronic ground state (X, $\nu = 1$) is presented. The spectrum in the J-X wavenumber range is too dense for assignment, while the I-X band, which is plotted on the same scale, is below the detection limit. The low intensity of this system is in agreement with the failure to observe the I-X electronic system using LIF as reported by Page et al.⁹ In contrast, I-X transitions are accessible by TC-RFWM. Selection of individual rotational lines by the probe laser simplifies the corresponding TC-RFWM spectra, which are obtained by scanning the pump wavelength. Only transitions

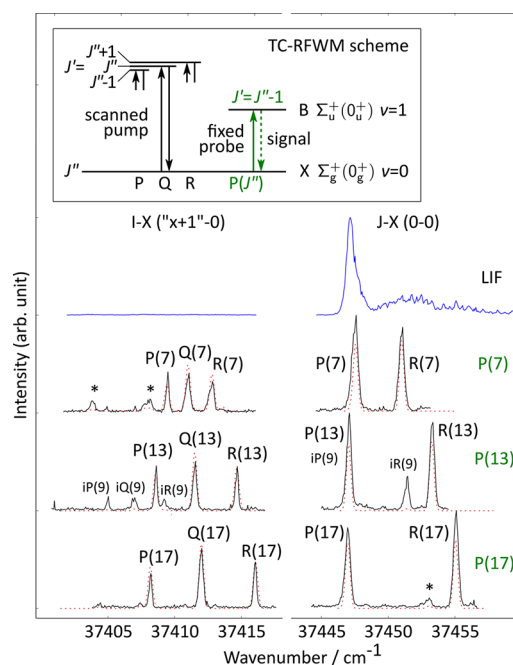


Figure 1. TC-RFWM spectra of the I-X and J-X transitions of $^{63}\text{Cu}_2$. The pump wavelength was scanned over the bands of interest while a single rotational line in the B-X (1–0) band (green label $P(J'')$) was probed. The inset illustrates this scheme that reduces the observed spectra to lines originating from a defined rotational level J'' of the ground state (X , $v = 0$). For comparison (and determination of lifetimes), dispersed fluorescence into the X , $v = 1$ level was recorded (blue excitation spectrum). Displayed on the same scale, virtually no dispersed fluorescence from the I state is visible. In the TC-RFWM spectra transitions to the I state are also weaker but clearly assignable. Overlaps of the probed B-X lines cause additional features (*) to appear. This is most apparent for the P(13) probe transition where overlap with the $iP(9)$ line of $^{63}\text{Cu}^{65}\text{Cu}$ adds additional features to the spectrum ($iP(9)$, $iQ(9)$, $iR(9)$); the label “i” is used to distinguish transitions of the isotopologue. The red dotted lines are simulations based on the fitted molecular constants. The presence of Q lines in the I-X transition allows assignment to a $^1\Pi_u(1_u)$ term symbol for the I state, and their absence in the J-X transition determines a $^1\Sigma_u^+(0_u^+)$ symbol for the J state.

that share the probed rotational level in the ground state produce signal. Therefore, even in the complex spectral regions of the band heads, the absorption spectrum is dramatically simplified and transitions can be assigned unambiguously.

The presence or absence of rotational Q lines in the I-X and J-X electronic systems, respectively, allows immediate assignment of the term symbol based on dipole selection rules. The spectrum of the I-X system corresponds to a $^1\Pi_u-1\Sigma_g^+$ transition, and the observed J-X transitions are in accordance with a $^1\Sigma_u^+-1\Sigma_g^+$ transition. Consequently the term symbol is $^1\Pi_u(1_u)$ for the I state and $^1\Sigma_u^+(0_u^+)$ for the J state. The treatment of Cu_2 in Hund's case a is under debate; therefore, Hund's case c labels were added in parentheses.

Tables S1 and S2 (see Supporting Information) contain 186 fitted line positions for transitions obtained by TC-RFWM scans. In addition, the corresponding lines in the (1–0) B-X band, which were used for selecting a rotational level J'' in the ground state, are listed. They cover the J-X (0–0) and (1–0) as well as the I-X (“x+1”–0) and (“x+2”–0) bands. The line positions were used to fit molecular constants for the individual bands using PGOPHER.¹² The residuals displayed in the third

column of the table denote the difference between the observed and the calculated line positions on the basis of the obtained molecular constants. For each band the origin T_v and rotational constant B_v were fitted. Higher-order distortions could not be fitted as no data for higher rotational quantum numbers (J') are available.

Table 1 displays the resulting molecular constants and the observed mean lifetimes. The lifetimes of the states were

Table 1. Molecular Constants and Lifetimes Obtained for the I and J States of $^{63}\text{Cu}_2$

J state	this work	literature
T_0 [cm^{-1}]	37448.765(12)	37451.1 ^a
T_1 [cm^{-1}]	37736.8868(91)	37738.4 ^a
B_0 [cm^{-1}]	0.115556(36)	
B_1 [cm^{-1}]	0.114233(17)	
lifetime [ns]	65.75(34)	80(10) ^b
I state	this work	Literature
T_{x+1} [cm^{-1}]	37410.7775(60)	37413.3 ^a
T_{x+2} [cm^{-1}]	37700.150(10)	37701.3 ^a
B_{x+1} [cm^{-1}]	0.112447(28)	
B_{x+2} [cm^{-1}]	0.112940(53)	
lifetime τ	$10 \text{ ps}^c \leq \tau \leq 5 \text{ ns}^d$	

^aPowers et al.⁸ ^bPage et al.⁹ ^cLower limit estimated by observed line width. ^dUpper limit estimated by comparison of dispersed LIF and excitation pulses. The vibrational numbering of the I state is not known; therefore, the labeling used by Powers et al.⁸ is adopted. One standard deviation in units of the last figure was appended in parentheses.

obtained by evaluation of the time dependence of the dispersed LIF signal. In case of the I-X transition 10 000 averages on the band head of the P branch were used to compensate for the low number of events. The excitation pulse duration of approximately 10 ns was too long for a precise measurement of the lifetime, but an upper limit of the mean lifetime could be estimated by fitting to the final decay of the averaged signal. A lower limit of the lifetime can be estimated from the observed line width, which is comparable to those of the long-living J state. The reason for the short lifetime is unclear, but predissociation effects could play a role. To assess the lifetime of the J state, a spectrally separated transition was chosen. The pump wavelength was tuned to the J-X (0–0) R(5) line of $^{63}\text{Cu}_2$, but some overlap with R(6) of the heavier isotopologue $^{63}\text{Cu}^{65}\text{Cu}$ cannot be ruled out. An exponential fit to the averaged LIF signal was used to estimate the mean lifetime.

Table 2 contains equilibrium molecular constants for the J state. They are estimated from the obtained constants for $v = 0$ and $v = 1$. The T_e and ω_e values are subject to comparatively large uncertainties, as they inherit the uncertainties of the literature value for $\omega_e x_e$.⁸ For the I state a similar procedure to obtain equilibrium constants is not applicable, because the absolute vibrational quantum numbers of the levels have not been determined.

As a consequence of the determined $^1\Sigma_u^+$ term symbol of the J state, its full electronic configuration can be established. Following the reasoning of Sappey et al.,¹³ the slightly higher vibrational constant of the J state (289 cm^{-1}) compared to the ground state X (266 cm^{-1})¹¹ suggests that the $4s\sigma^2$ bond of the ground state remains intact on excitation. As a consequence, the J-X transition involves the promotion of a 3d electron into a slightly bonding or nonbonding orbital. This promotion is

Table 2. Derived Equilibrium Constants for the J State of $^{63}\text{Cu}_2$

J state	this work	literature
T_e [cm^{-1}]	37437.20(33) ^a	37437.7(1) ^{b,f}
ω_e [cm^{-1}]	289.40(88) ^a	288.4(21) ^c
B_e [cm^{-1}]	0.116218(54)	0.1165(5) ^b
α_e [cm^{-1}]	0.001323(40)	0.0010(5) ^b
r_e [\AA]	2.14708(50)	2.15 ^b
$\Delta G_{1/2}$ [cm^{-1}]	288.121(15) ^d	287.3 ^e

^aCalculated using $\omega_e x_e = 0.64(44) \text{ cm}^{-1}$ from Powers et al.⁸ ^bPage et al.⁹ ^cPowers et al.⁸ ^dCalculated as $T_1 - T_0$. ^eCalculated as $T_1 - T_0$ using the values reported by Powers et al.⁸ ^fSeems to neglect propagation of uncertainty.

likely into a 4p molecular orbital, as the energy involved is comparable to the one for a 4p-3d transition in atomic Cu. Also, the diabatic dissociation energy of a Morse potential, which is determined by the molecular constants of the J state, is in the range of the $3d^9 4s 4p + 3d^{10} 4s$ asymptotes. Experimentally, Sappey et al. observed direct photoionization of the J state of Cu_2 to form a $^2\Pi$ state of Cu_2^+ in a facile, one-electron process. This can be attributed to the photoejection of the electron in a 4p molecular orbital, while the $3d\pi$ hole of this ion state is already present in the J state of Cu_2 . Therefore, out of the molecular orbitals with predominantly 4p character, only the slightly bonding $4p\sigma_g$ and $4p\pi_u$ orbitals remain as possible targets for the promoted $3d\pi$ electron. Hence, Sappey et al. conclude that the Hund's case a description of the J state is either $^1\Pi_u$ from $3d^{18} 3d\pi_u 4s\sigma_g^2 4p\sigma_g$ or $^1\Sigma_u^+$ from $3d^{18} 3d\pi_g 4s\sigma_g^2 4p\pi_u$ ($3d^{18}$ denotes nine doubly occupied 3d molecular orbitals). This work's unambiguous assignment of the J state to $^1\Sigma_u^+$ allows determination of the electronic configuration of the J state as $3d^{18} 3d\pi_g 4s\sigma_g^2 4p\pi_u$.

CONCLUSIONS

The applicability of TC-RFWM for spectral simplification was demonstrated on UV transitions of the neutral copper dimer. Lines of individual isotopologues were identified by double-resonant labeling of individual rotational levels. Also, some lines, otherwise buried in band heads, were resolved. In this way, TC-RFWM has been shown to conclusively answer questions on the term symbols of the addressed states that were left open for three decades. In this study, the I state was rotationally resolved for the first time. Previous LIF measurements were hampered by the low fluorescence yield of this state.⁹ Observation of Q lines in the I-X transition allowed assignment of the term symbol of the I state to $^1\Pi_u(1_u)$. Term energies and rotational constants for two vibrational levels are provided. The mean lifetime of the I state was inferred to lie between 10 ps and 5 ns. No Q lines were observed in the J-X transition. Therefore, the J state could be assigned to $^1\Sigma_u^+(0_u^+)$. Analysis of the two lowest vibrational levels also allowed refinement of the equilibrium constants and the mean lifetime provided by literature. Finally, by determining the $^1\Sigma_u^+$ character of the J state, the parity of its $3d\pi$ -hole¹³ could be decided. On the basis of the candidates identified by Sappey et al.,¹³ the complete configuration of the J state of Cu_2 is $3d^{18} 3d\pi_g 4s\sigma_g^2 4p\pi_u$.

ASSOCIATED CONTENT

Supporting Information

The Supporting Information is available free of charge on the ACS Publications website at DOI: 10.1021/acs.jpca.7b09838.

Line lists (PDF)

AUTHOR INFORMATION

Corresponding Author

*E-mail: peter.radi@psi.ch.

ORCID

M. Beck: 0000-0002-4475-3587

B. Visser: 0000-0002-9798-3079

P. Bornhauser: 0000-0003-1293-2668

G. Knopp: 0000-0002-0786-3402

J. A. van Bokhoven: 0000-0002-4166-2284

P. P. Radi: 0000-0003-1197-1091

Notes

The authors declare no competing financial interest.

ACKNOWLEDGMENTS

This work is supported by Swiss National Science Foundation (# 200021_153170).

REFERENCES

- Groothaert, M. H.; Smeets, P. J.; Sels, B. F.; Jacobs, P. A.; Schoonheydt, R. A. Selective Oxidation of Methane by the Bis(μ -oxo)copper Core Stabilized on ZSM-5 and Mordenite Zeolites. *J. Am. Chem. Soc.* **2005**, *127*, 1394–1395.
- Lieberman, R. L.; Rosenzweig, A. C. Crystal Structure of a Membrane-Bound Metalloenzyme that Catalyses the Biological Oxidation of Methane. *Nature* **2005**, *434*, 177–182.
- Himes, R. A.; Barnese, K.; Karlin, K. D. One is Lonely and Three is a Crowd: Two Coppers Are for Methane Oxidation. *Angew. Chem., Int. Ed.* **2010**, *49*, 6714–6716.
- Morse, M. D. Chemical Bonding in the Late Transition Metals: The Nickel and Copper Group Dimers. In *Advances in Metal and Semiconductor Clusters*; Duncan, M. A., Ed.; JAI Press: Greenwich, 1993; Vol. 1, pp 83–121.
- Okazaki, T.; Ando, Y. New Optical Absorption Spectra of Cu_2 Molecules Produced by the Gas Evaporation Technique. *Mol. Phys.* **2000**, *98*, 447–452.
- Lecoultre, S.; Rydlo, A.; Felix, C.; Buttet, J.; Gilb, S.; Harbich, W. Optical Absorption of Small Copper Clusters in Neon: Cu_n ($n = 1-9$). *J. Chem. Phys.* **2011**, *134*, 074303.
- Parry, I. S.; Hermes, A. C.; Kartouzian, A.; Mackenzie, S. R. Imaging the Photodissociation Dynamics of Neutral Metal Clusters: Copper Dimer, Cu_2 , and Copper Oxide, CuO . *Phys. Chem. Chem. Phys.* **2014**, *16*, 458–466.
- Powers, D. E.; Hansen, S. G.; Geusic, M. E.; Michalopoulos, D. L.; Smalley, R. E. Supersonic Copper Clusters. *J. Chem. Phys.* **1983**, *78*, 2866–2881.
- Page, R. H.; Gudeman, C. S. Rotationally Resolved Dicopper (Cu_2) Laser-Induced Fluorescence-Spectra. *J. Chem. Phys.* **1991**, *94*, 39–51.
- Visser, B.; Beck, M.; Bornhauser, P.; Knopp, G.; Gerber, T.; Abela, R.; van Bokhoven, J. A.; Radi, P. P. Unraveling the Electronic Structure of Transition Metal Dimers using Resonant Four-Wave Mixing. *J. Raman Spectrosc.* **2016**, *47*, 425–431.
- Ram, R. S.; Jarman, C. N.; Bernath, P. F. Fourier-Transform Emission-Spectroscopy of the Copper Dimer. *J. Mol. Spectrosc.* **1992**, *156*, 468–486.
- Western, C. M. *PGOPHER, version 10.0*; University of Bristol Research Data Repository: Bristol, 2017; DOI: 10.5523/bris.160i6ix-oo4kir1jxvawfws047m.

(13) Sappey, A. D.; Harrington, J. E.; Weisshaar, J. C. Resonant Two-Photon Ionization-Photoelectron Spectroscopy of Cu_2 : Autoionization Dynamics and Cu_2^+ Vibronic States. *J. Chem. Phys.* **1989**, *91*, 3854–3868.